AJNR

In vitro evaluation of MR hypointensity in Aspergillus colonies.

D W Fellows, V D King, T Conturo, R N Bryan, W G Merz and S J Zinreich

AJNR Am J Neuroradiol 1994, 15 (6) 1139-1144
http://www.ajnr.org/content/15/6/1139

In Vitro Evaluation of MR Hypointensity in *Aspergillus* Colonies

D. W. Fellows, V. D. King, T. Conturo, R. N. Bryan, W. G. Merz, and S. J. Zinreich

PURPOSE: To demonstrate that paramagnetic elements in fungal colonies can cause hypointensity in MR images. **METHODS:** *Aspergillus fumigatus* grown in vitro was imaged with CT and MR at the time of initial inoculation and 5 days later. CT and MR images, T2 values, scanning electron microscopy, energy-dispersive analysis, and furnace atomic absorption spectrometry were performed. **RESULTS:** After 5 days of growth, MR images of *A fumigatus* revealed curvilinear hypointensities on T2-weighted images corresponding to the fungal growth. Gradient-echo images revealed two distinct components of hypointensity with different calculated T2 values. Phase-angle-difference images revealed a phase shift characteristic of magnetic-susceptibility paramagnetic effects, which corresponded to the hypointense regions on gradient-echo images. Energy-dispersive analysis and furnace atomic absorption spectrometry confirmed the presence of paramagnetic elements. **CONCLUSION:** It was shown that in vitro *A fumigatus* concentrates metal elements contained within the nutrient broth. These focal collections of calculated T2 values are caused at least partly by magnetic susceptibility effects.

Index terms: Aspergillosis; Magnetic resonance, experimental; Magnetic resonance, tissue characterization; Paranasal sinuses, magnetic resonance

AJNR Am J Neuroradiol 15:1139–1144, Jun 1994

Magnetic resonance (MR) imaging has significantly improved relative contrast between various normal and abnormal soft tissues. Within the nasal cavity and paranasal sinuses it was hoped that it might aid in the distinction of disease. Earlier publications have discussed MR's ability to differentiate fungal sinusitis from bacterial and viral inflammatory disease and neoplasms (1–3). Zinreich et al suggested that the distinct low signal appearance of fungal sinusitis was caused by the presence of ferromagnetic elements such as iron, magnesium, and manganese (1). However, Som et al contended that at least part of the explanation of the low signal seen was a dehydration effect that occurs in chronic inflammatory disease (2). To gain a better understanding of the appearance of fungal concretions on MR, and the potential role of paramagnetic elements, we performed a series of in vitro experiments. Our purpose was to demonstrate, experimentally, that paramagnetic elements could cause hypointensity in MR images of *Aspergillus* colonies.

We hypothesized that *Aspergillus* organisms must accrue concentrations of paramagnetic elements and that these paramagnetic elements pro-

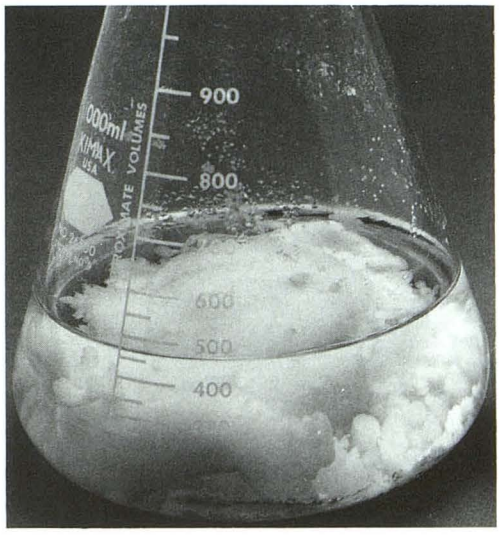

Fig. 1. Flask containing the hyphal mass after 5 days of growth in the nutrient broth.

Received May 4, 1993; accepted after revision December 23.

From the Russell H. Morgan Department of Radiology (D.W.F., T.C., R.N.B., S.J.Z.) and the Department of Pathology (D.K., W.G.M.), Johns Hopkins Medical Institutions, Baltimore.

Address reprint requests to D. W. Fellows, Russell H. Morgan Department of Radiology and Radiological Sciences, Johns Hopkins Medical Institutions, 600 N Wolfe St, Baltimore, MD 21205.

AJNR 15:1139–1144, Jun 1994 0195-6108/94/1506–1139

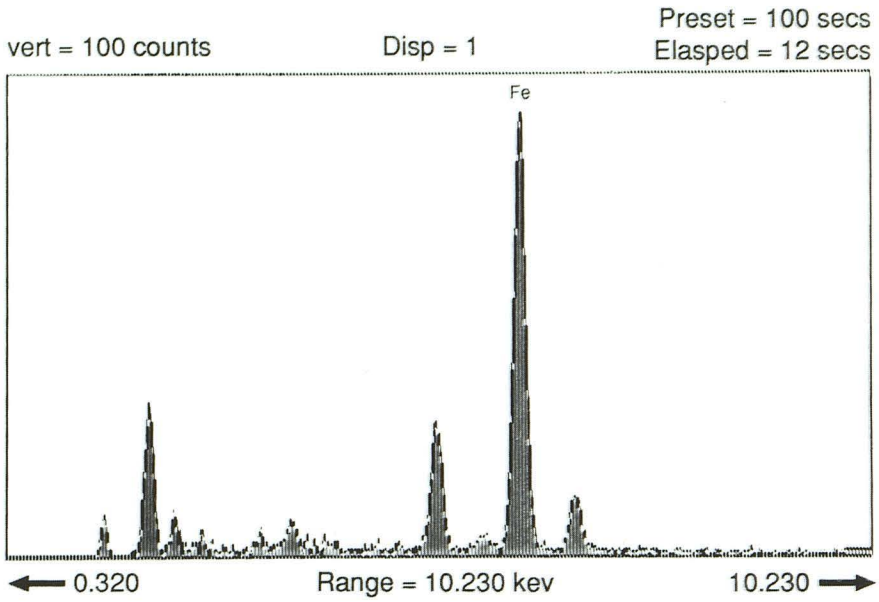

Fig. 2. Results of energy-dispersive analysis showing the energies of characteristic x-rays from specific elements in the sample. Prominent peaks from iron are labeled.

TABLE 1: Furnace atomic absorption spectroscopy

Element	Concentration ($\mu g/g$)
Iron	1096
Magnesium	2393
Manganese	163
Zinc	44

TABLE 2: Concentration of iron and magnesium in sabouraud dextrose broth and normal serum

	Sabouraud Dextrose Broth (mg/L)	Serum (mg/L)
Iron	0.33	0.6–1.5
Magnesium	5.6	18–30

duce local changes in magnetic susceptibility resulting in signal loss on MR images. Our aims therefore, were to: *(a)* confirm the presence and measure the concentration of paramagnetic elements within fungal colonies; *(b)* document signal loss on T2-weighted spin echo images of fungal colonies and *(c)* Demonstrate that signal loss is caused by a T2* effect on magnetic susceptibility-weighted images.

Materials and Methods

Isolates of *Aspergillus fumigatus* were grown on Sabouraud dextrose agar slants for 8 days at 25°C with the resulting growth then suspended in 5 mL of 1% percent Tween 80. The suspension was then introduced into 750 mL of Sabouraud dextrose broth (Bacto-Peptone 10 g/L, Difco Laboratories, Detroit, Mich; d-glucose 20 g/L, Sigma Chemical Company, St. Louis, Mo) and grown at 28°C with contrast agitation for an additional 5 days. Sabouraud dextrose broth is a standard growth medium, but it is a commercial proprietary broth and its exact chemical composition is not fully defined. The flask containing the suspension of *A fumigatus* was evaluated with computed tomography and MR immediately after the initial suspension was added to the Sabouraud broth and again after the 5 days of growth in that medium.

After the 5 days of growth, multiple samples from the fungal mass were evaluated with a Hitachi (Tokyo, Japan) S-570 scanning electron microscope. Specific elements within the fungal mass were identified with a Kevex (San Carlos, Calif) energy-dispersive analyzer. In addition, a sample of the fungal mass was removed and washed in phosphate-buffered saline and then evaluated with furnace atomic absorption spectrometry for the presence of iron, magnesium, manganese, and zinc.

Computed tomographic scans were obtained on a GE 9800 unit (GE Medical Systems, Milwaukee, Wis). MR images were obtained on a Signa (GE Medical Systems) 1.5-T unit with the following parameters: spin-echo proton (^{1}H) images with the T1-weighted images 450/11/1 (repetition time/echo time [TE]/excitations); and double-echo images 3000/16, 30, or 100. The acquisition matrix was 256 × 256. Gradient-echo images 50/10,15,20,25,30 were acquired with a flip angle of 20° and 30°. Images were reconstructed from raw data using custom software. Phase-angle-difference images, representing a map of field strength, were then obtained by subtracting gradient-echo phase-angle images with an TE of 10 msec from gradient-echo phase-angle images with progressively larger TE values (4–6). By calculating phase-shift images from different TE intervals, baseline phase shifts caused by radio frequency field inhomogeneity were reduced. However, baseline phase shifts caused by static field inhomogeneity persisted.

To quantify T2 values, region of interest signal intensities were recorded at TEs of 30 and 100 msec from 34 separate sites. Calculations of T2 values were performed using standard GE Signa software for T2 measures.

TABLE 3: Calculated T2 values

	Mean (msec)	SD
Component 1	208.5	±6.2
Component 2	247.2	±13.0

Results

Computed tomographic scanning was performed on the Sabouraud broth immediately after adding the *A fumigatus* suspension, and an MR image was obtained immediately thereafter. On visual examination the Sabouraud broth revealed a clear medium without any internal structure. The computed tomographic and MR images did not reveal focal increased or decreased densities or signal intensities within the medium. Direct visual examinations 5 days later, during which time the flask containing the medium remained

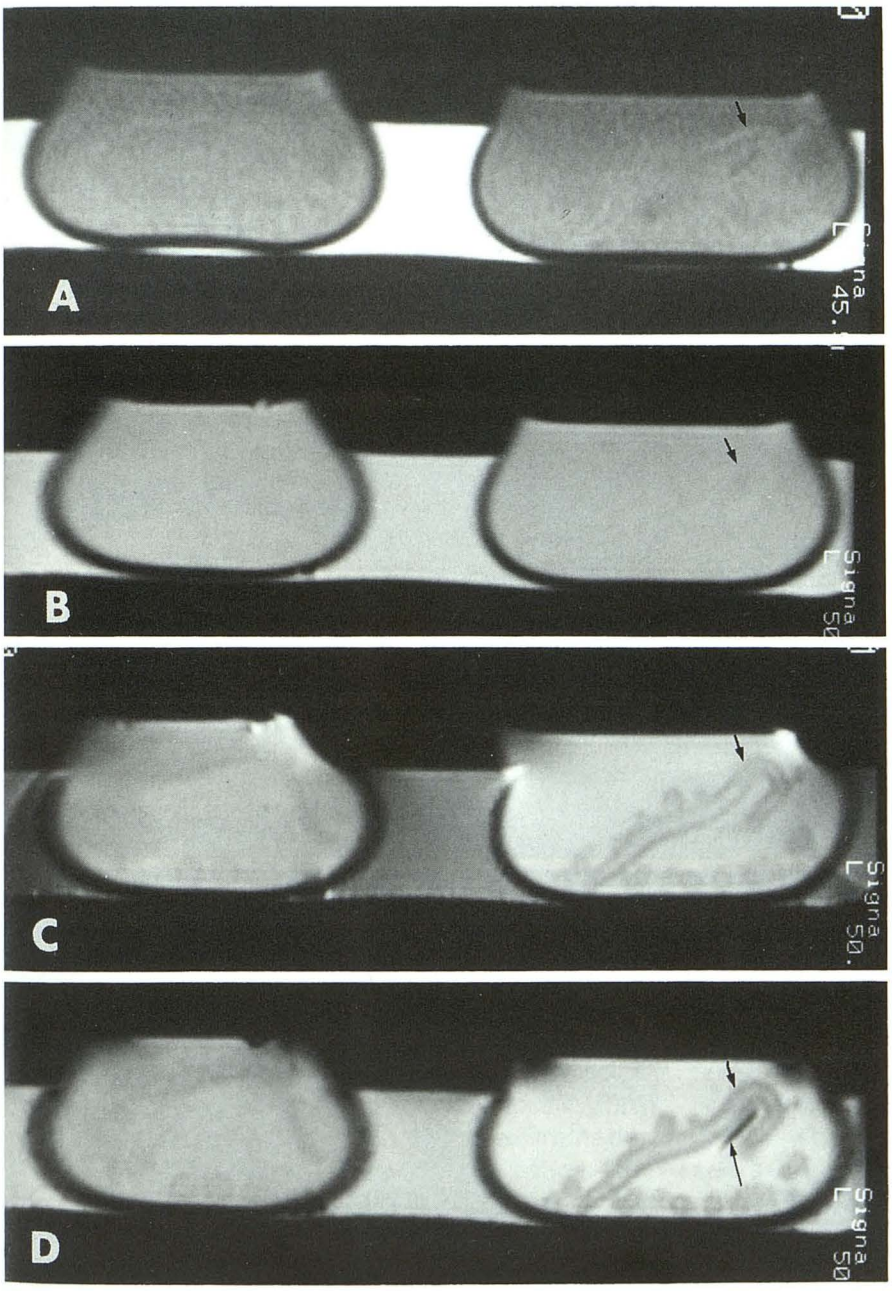

Fig. 3. Composite photograph of the appearance of *Aspergillus* hyphal mass on MR.

A, T1-weighted (450/11) image reveals a slightly hyperintense curvilinear (*arrow*) pattern corresponding to the hyphal mass.

B, Spin density–weighted (300/16) image shows only subtle hypointensity *(arrow)*.

C, T2-weighted (300/100) images show a hypointense curvilinear (*arrow*) pattern.

D, Gradient-echo (33/13, 30° flip angle) shows two distinct levels of hypointensity (*arrow*).

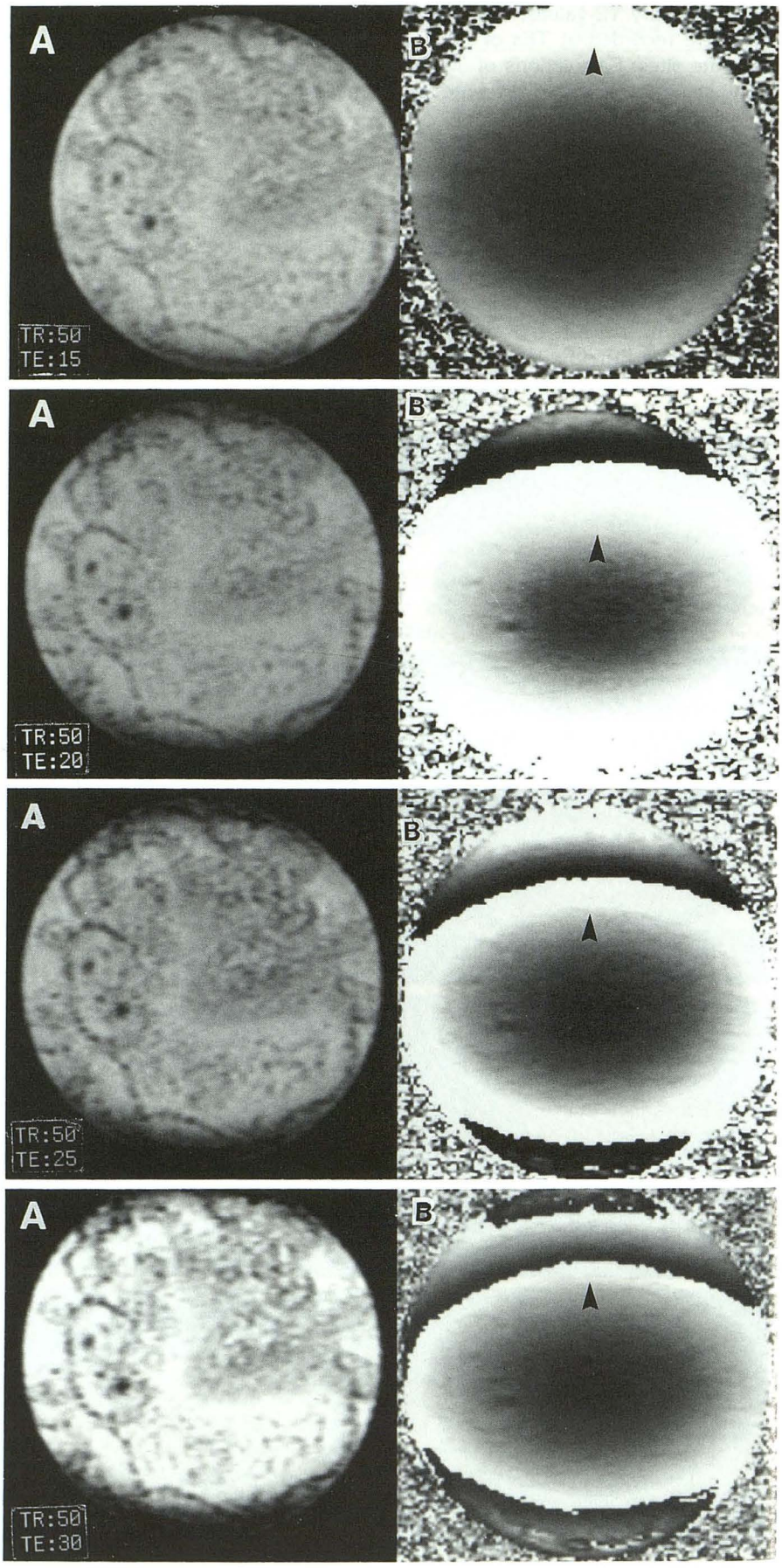

Fig. 4. Gradient-echo images (50/15,20,25,30; 20° flip angle) *(A)* and corresponding phase-angle difference images *(B)* show that net phase shift increases with increases in TE. Concentric rings (*arrowheads*) on phase-angle difference images are caused by field inhomogeneity; focal phase shift is caused by paramagnetic effects. A reference image having a TE of 10 msec (not shown) was used as the reference for all phase subtractions.

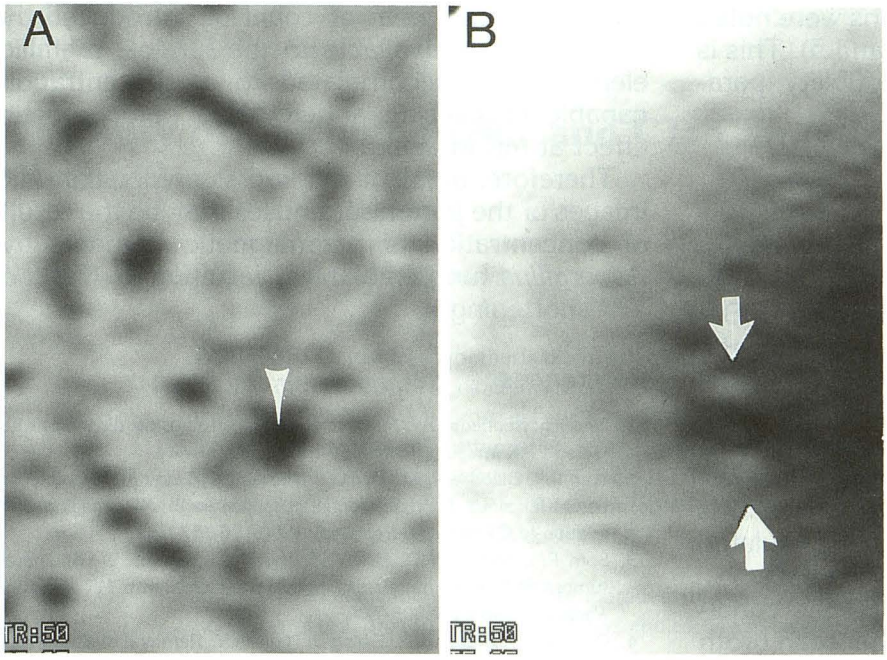

Fig. 5. Magnified gradient-echo (50/25, 20° flip angle) image *(A)* and corresponding phase-angle image *(B)*. Note that phase shift corresponds to focal area of signal loss (*arrowhead*) on the gradient-echo image. The two bright crescents (*arrows*) are characteristic of magnetic susceptibility paramagnetic effects.

sealed, revealed a globular hyphal mass within the growth medium (Fig 1). Light and scanning electron microscopy of this mass revealed hyphae and conidiophores characteristic of *Aspergillus* organisms. Specific elements within the fungal sample were identified using the Kevex energy-dispersive analyzer by characteristic x-rays unique to the particular elements contained within the sample. Focal areas containing iron and magnesium were identified (Fig 2). Furnace atomic absorption spectrometry revealed the concentrations of iron and magnesium to be 1096 μg/g and 2393 μg/g, respectively. Manganese and zinc were also found but in much smaller quantities (Table 1). It should be noted that the concentration of these elements within the Sabouraud broth was less than the physiologic concentrations of these elements in normal human serum (Table 2) (7). As the concentration of paramagnetic elements in the solution increases, the *A fumigatus* should accrue greater concentrations of these elements, as has been demonstrated with other fungi (6).

MR imaging of the 5-day *A fumigatus* growth revealed a curvilinear pattern of hyperintense signal on T1-weighted images relative to the low signal broth (Fig 3A), corresponding to the form of the hyphal mass seen with visual examination of the flask. On the T2-weighted image, the central portion of the above described curvilinear pattern had a low signal intensity (Fig 3C). Several of these T2-weighted images suggested the presence of two *degrees* of hypointensity. The gradient-echo T2*-weighted images revealed more clearly the presence of two distinct *components* of hypointensity (Fig 3D). The more hypointense component was labeled component 1 and had a mean calculated T2 value of 208.5 (±6.2) msec. Component 2 (the less hypointense region) had a mean calculated T2 value of 247.2 (±13.0) msec (Table 3).

Gradient-echo images were acquired with progressively longer TE values. Regions of signal loss were demonstrated; however, this appearance is nonspecific and could be the result of decreased proton densities and T2 and/or T2* effects, any of which could occur in inspissated secretions. Demonstration of a net phase shift as a function of TE on these images would be more specific for paramagnetic susceptibility effects. By increasing the TE, we caused an increase in the phase-angle shift in an area of altered local magnetic susceptibility. Variations in the field caused by inhomogeneity of the magnet are seen as concentric rings in the phase shift images (Figs 4 and 5). Focal phase-shift heterogeneity is specific for magnetic susceptibility paramagnetic effects (4, 6) (Figs 4 and 5). The amount of shift corresponds to the change in magnetic susceptibility, which is related to the concentration of the paramagnetic element. The geometry of the distortion is also specific for a paramagnetic collection. In this case, we see the characteristic pattern of two bright crescents oriented along the z-axis.

Two less visible hypointensity regions were noted perpendicular to the Z axis (Figs 4 and 5). This is characteristic for magnetic susceptibility paramagnetic effects.

Discussion

To understand the possible role of paramagnetic elements within *Aspergillus* colonies, a series of in vitro experiments were performed. Before the growth of the fungus, paramagnetic elements were not concentrated enough to be detected on MR images. After 5 days of growth, *A fumigatus* accrued concentrations of the metal elements contained within the broth. Furthermore, local collections of paramagnetic elements were demonstrated to have decreased calculated T2 values and magnetic susceptibility effects.

This in vitro experiment simulated the conditions present in fungal sinusitis. Rather than broth with paramagnetic elements, hyperemic inflammatory mucosa would result in increased serum in the tissues with the serum having greater concentrations of paramagnetic elements than broth.

However, the precise source of the metallic elements accumulated by the fungus in a clinical situation remains unclear. These paramagnetic elements could pass from the inflamed mucosa into the sinus lumen or could be introduced by air flow. Once available to the fungus, metallic elements are accumulated to a concentration capable of causing a detectable paramagnetic effect at MR imaging.

Therefore, areas of marked signal loss on MR images of the paranasal sinuses may be the result of concentration of paramagnetic elements by *Aspergillus* fungal colonies, resulting in T2 and T2* shortening.

References

1. Zinreich, Kennedy DW, Malat J, et al. Fungal sinusitis: diagnosis with CT and MR imaging. *Radiology* 1988;169:439–444
2. Som PM, Dillon WP, Curtin HD, Fullerton GD, Lidov M. Hypointense paranasal sinus foci: differential diagnosis with MR imaging and relation to CT findings. *Radiology* 1990;176:777–781
3. Som PM, Shapiro MD, Biller HF, Sasaki C, Lawson W. Sinonasal tumors and inflammatory tissues: differentiation with MR imaging. *Radiology* 1988;167:803–808
4. Ordidge RJ, Branch CA, Ewing J, Nagesh V. Removal of the effects of global magnetic field inhomogeneity in heavily T2*-weighted MR images. *J Magn Reson Imaging* 1993;3:120–123
5. Conturo TE, Barker PB, Mathews VP, Monsein LH, Bryan RN. MR imaging of cerebral perfusion by phase-angle reconstruction of bolus paramagnetic-induced frequency shifts. *Magn Reson Med* 1992;27:375–390
6. Ro YM and Cho ZH. A new frontier of blood imaging using susceptibility effect and tailored RF pulses. *Magn Reson Med* 1992;28: 237–248
7. Tietz NW. *Fundamentals of clinical chemistry*. 3rd ed. Philadelphia: Saunders, 1987:952–959